

Slip and flow of hard-sphere colloidal glasses

P. Ballesta^{1,2}, R. Besseling¹, L. Isa¹, G. Petekidis² and W. C. K. Poon¹

¹*Scottish Universities Physics Alliance (SUPA) and School of Physics, The University of Edinburgh, Kings Buildings, Mayfield Road, Edinburgh EH9 3JZ, United Kingdom.*

²*IESL-FORTH and Department of Materials Science and Technology, University of Crete, Heraklion 71110, Crete, Greece*

(Dated: February 6, 2020)

We study the flow of concentrated hard-sphere colloidal suspensions along smooth, non-stick walls using cone-plate rheometry and simultaneous confocal microscopy. In the glass regime, the global flow shows a transition from Herschel-Bulkley behavior at large shear rate to a characteristic Bingham slip response at small rates, absent for ergodic colloidal fluids. Imaging reveals both the ‘solid’ microstructure during full slip and the local nature of the ‘slip to shear’ transition. Both the local and global flow are well described by a phenomenological model, and the associated Bingham slip parameters exhibit characteristic scaling with size and concentration of the hard spheres.

PACS numbers: 82.70.y, 83.50.-v, 83.60.-a, 83.85.Ei

Wall slip in fluid flow has received considerable attention for many years [1, 2, 3, 4, 5, 6, 7, 8, 9, 10, 11, 12, 13]. Even for simple fluids it has been realized that the no-slip boundary condition may not be an accurate description on the small length scales relevant for nanoporous media or nanofluidics [1]. More widespread, and of even greater practical relevance, is the presence of slip in complex fluids like suspensions and emulsions [2, 3, 4, 5, 6, 7, 8, 9, 10, 11, 12, 13]. Despite the more accessible length scales in these systems, it has remained challenging to obtain microscopic insight into the nature of slip and understand its dependence on material composition, wall properties and flow rate. Recently, considerable progress has been made for soft particle pastes and emulsions [7], but for hard particle suspensions the situation remains unclear. Slip was observed both in solid- [11, 12] and liquid-like [13, 14] suspensions of this kind, but its possible relation to Brownian motion and the glass transition was mostly ignored.

Experimentally, a proper interpretation of slip requires not only precise rheological data but also detailed spatial characterization of the flow. Various imaging methods have been employed the last decades [5, 7, 13, 14, 15, 16, 17]; however they either lack the resolution to study flow near the wall on the single particle level [5, 7, 13, 14, 15], or they do not provide simultaneous rheological and microscopic information on the same sample [16, 17].

In this Letter, we employ confocal imaging in a cone-plate rheometer to address the slip and yielding of concentrated hard-sphere (HS) colloids simultaneously on the microscopic and the macroscopic scales. Slip appears with the emergence of a yield stress on entering the glass regime, with plug-flow persisting down to the single particle-wall interface. We find that the slip response is Bingham-like, which is very different from what was found for emulsions [7]. Thus, in contrast to a recent suggestion [7], the physics of slip is *not* universal between different classes of soft glassy materials.

We used polymethylmethacrylate (PMMA) colloids of various radii ($a = 138$ nm, 150 nm, 302 nm, polydispersity $\sim 15\%$, all from light scattering), stabilized with chemically-grafted poly-12-hydroxystearic acid, suspended in a mixture of decalin and tetralin (viscosity $\eta_s = 2.3$ mPas) for refractive index (RI) matching and seeded with $\sim 0.5\%$ of fluorescent particles of the same kind ($a = 652$ nm) for confocal imaging. In these solvents, the interparticle interaction is very nearly HS-like [18]. Batches of different volume fractions ϕ were prepared by diluting samples centrifuged to a random close packed sediment, taken to be at $\phi_{\text{rcp}} = 0.67$ [19]. When comparing data from different particle sizes, however, we report results in the reduced variable $1 - \phi/\phi_{\text{rcp}}$, which is independent of the numerical value taken for ϕ_{rcp} .

Measurements were performed in a controlled stress rheometer (AR2000, TA Instr.) in cone-plate geometry (radius $r_c = 20$ mm, cone angle $\theta = 1^\circ$) with a modified base on which a glass slide (radius 25 mm, thickness ~ 180 μm [20], local roughness < 1 nm from AFM) is mounted. A solvent trap minimizes evaporation. By coupling in a piezo-mounted objective ($\geq 60\times$, oil immersion) and optics via an adjustable arm connected to a confocal scanner (VT-Eye, Visitech Int.) we measure the velocity profile $v(z, r)$ (with z the velocity-gradient direction) from movies taken at $\delta z = 2\text{--}5$ μm intervals at a frame rate ≤ 90 Hz at various distances r from the cone center, Fig. 1(a). To prevent slip, both the glass and the cone can be made rough on the particle scale by spin-coating a $\phi \sim 0.3$ suspension and sintering the resulting disordered colloidal monolayer. Experiments with both the smooth and the coated glass plates were performed; the cone is always coated to ensure stick boundary conditions at the top. All data were collected with controlled applied shear rate $\dot{\gamma}_a$ (moving from high to low $\dot{\gamma}_a$) but stress controlled measurements gave the same results.

We first discuss how the rheology depends on ϕ and the wall conditions. Figure 1(b) shows the measured stress

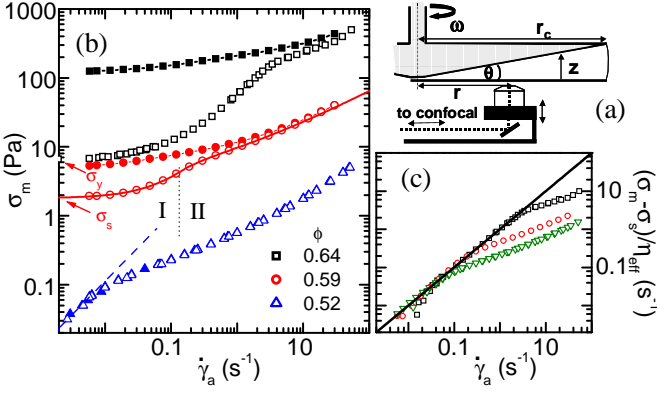


FIG. 1: (a) Setup: cone-plate rheometer with transparent base and optics connected via an adjustable arm to the confocal scanner. (b) Measured stress σ_m versus applied rate $\dot{\gamma}_a$ for particles with $a = 138$ nm, at different volume fractions for coated (■, ●, ▲) and un-coated geometries (□, ○, △). Dashed line: linearly viscous behavior. Full line: σ_m from Eq. (4) for $\phi = 0.59$, using Eq. (5) for $r > r_y(\dot{\gamma}_a)$ (see text) and parameters $\sigma_s = 1.8$ Pa, $\beta = 8.2 \cdot 10^4$ Pa s m $^{-1}$, $\sigma_y = 5.5$ Pa and $\alpha = 6.1$ Pa s $^{1/2}$. Dotted line: critical applied rate $\dot{\gamma}_{a,c}$ (see text). (c) Reduced stress $(\sigma_m - \sigma_s)/\eta_{\text{eff}}$ versus $\dot{\gamma}_a$ for $\phi = 0.58$ (▽), 0.59 (○), and 0.64 (□). Full line: $(\sigma_m - \sigma_s)/\eta_{\text{eff}} = \dot{\gamma}_a$.

σ_m versus $\dot{\gamma}_a$ for coated and uncoated glass slides at various ϕ for $a = 138$ nm. For a concentrated fluid ($\phi = 0.52$) below the colloidal glass transition ($\phi_g \simeq 0.57$ from mean squared displacement measurements) we find linear behavior (viscous flow) at the smallest $\dot{\gamma}_a$ and shear thinning at higher $\dot{\gamma}_a$, independent of boundary condition.

However, for $\phi > \phi_g$ the coated and uncoated results differ markedly. With coating, we find (as before, [21]), Herschel-Bulkley (HB) behavior: $\sigma_m = \sigma_y + \alpha \dot{\gamma}_a^n$, with σ_y the yield stress [22]. On the other hand, for the smooth surface, $\sigma_m(\dot{\gamma}_a)$ shows two regimes. For stresses well below σ_y , we find apparent flow described by $\sigma_m = \sigma_s + \eta_{\text{eff}} \dot{\gamma}_a$, Fig. 1(c), with a threshold σ_s and an effective viscosity η_{eff} (regime I). As shown below, this corresponds to full wall-slip and solid-body rotation of the sample over the entire geometry. This ‘Bingham’ slip differs from non-Brownian suspensions [12, 13], where no threshold σ_s is seen. It is also distinct from the behavior $\sigma_m - \sigma_s \propto \sqrt{\dot{\gamma}_a}$ in soft particle pastes [7]. For larger stresses (regime II), $\sigma_m(\dot{\gamma}_a)$ with smooth glass deviates from the Bingham form, the sample starts to yield and σ_m approaches the HB curve.

To check whether the slip in regime I reflects full sliding from the first colloid layer or, instead, local yielding on the scale of a few particles near the surface, we used the fully fluorescent batch ($a = 652$ nm) and performed three-dimensional imaging and particle tracking [24] of the flow starting directly above the glass. The density profile for $\phi = 0.63$ in Fig. 2(a) shows that the surface induces layering, despite the polydispersity. Nevertheless, the corresponding *microscopic* velocity profile, also

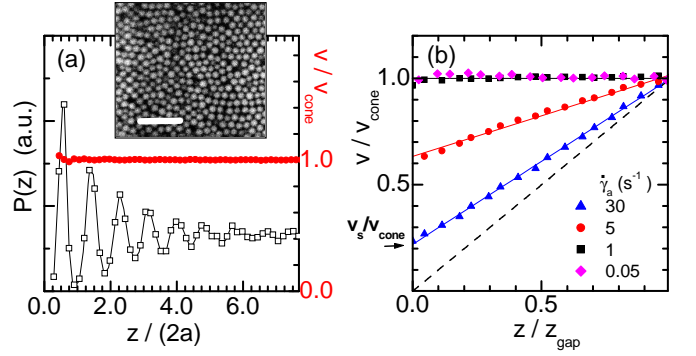


FIG. 2: (a) Density profile $P(z)$ (□), from 3D-imaging of the $a = 652$ nm system at $\phi = 0.63$, during slip at $r = 2.5$ mm and $\dot{\gamma}_a = 0.01$ s $^{-1}$. (●) Corresponding velocity profile from particle tracking, showing full plug flow. Inset: Slice of one of the 3D-images, showing the first colloid layer. Scale bar: 10 μm . (b) Velocity profiles for the $\phi = 0.59$ data in Fig. 1(b), in units of the cone velocity $v_{\text{cone}} = \dot{\gamma}_a \theta r$, as function of the normalized height $z/z_{\text{gap}} = z/\theta r$, for various applied rates $\dot{\gamma}_a$ at $r = 2.5$ mm. The arrow marks the slip velocity for $\dot{\gamma}_a = 30$ s $^{-1}$; the dashed line shows the behavior without slip $v = \dot{\gamma}_a z$ as observed for $\phi < \phi_g$ or in newtonian liquids.

shown in Fig. 2(a), evidences complete sliding with respect to the glass, with $v = v_{\text{cone}}$ down to the first layer. Further analysis (data not shown) confirmed that particles remained caged and that yielding was absent.

We now turn to the velocity profiles associated with the rheology in Fig. 1(b). Figure 2(b) shows $v(z)$ normalized by v_{cone} at a distance $r = 2.5$ mm from the center of the cone for $\phi = 0.59$ at various $\dot{\gamma}_a$. We observe linear profiles for all $\dot{\gamma}_a$ but with a finite slip velocity, defined as the $z = 0$ intercept of $v(z)$, and a slope corresponding to a bulk shear rate $\dot{\gamma} < \dot{\gamma}_a$. On reducing $\dot{\gamma}_a$, the profiles show increasing slip and, for the lowest applied rates, $\dot{\gamma}$ vanishes, giving $v(z) = v_{\text{cone}}$ [23].

As seen for the profile at $\dot{\gamma}_a = 1$ s $^{-1}$ in Fig. 2(b), plug flow can occur locally even when the global flow curve is close to that found for rough walls. To bring out the behavior as function of r when entering regime II, we show in Fig. 3(a) the local shear rate obtained from imaging at various distances r at fixed $\dot{\gamma}_a = 1.1$ s $^{-1}$. Solid body rotation ($\dot{\gamma} = 0$) occurs at small r , while $\dot{\gamma} > 0$ for larger r . This shows directly that, at fixed $\dot{\gamma}_a$, the stress is r -dependent and decreases for smaller r [3].

The local and global rheology described above can be rationalized using a simple model similar to [3, 12]. First, as suggested by the phenomenology of the data in Figs. 1(b),(c), we relate the local stress σ to the slip velocity v_s of the colloids along the wall by:

$$\sigma = \sigma_s + \beta v_s, \quad (1)$$

with a hydrodynamic term βv_s and a threshold stress σ_s . For the bulk flow, we use the HB form with $n = 0.5$:

$$\sigma = \sigma_y + \alpha \dot{\gamma}^{0.5}. \quad (2)$$

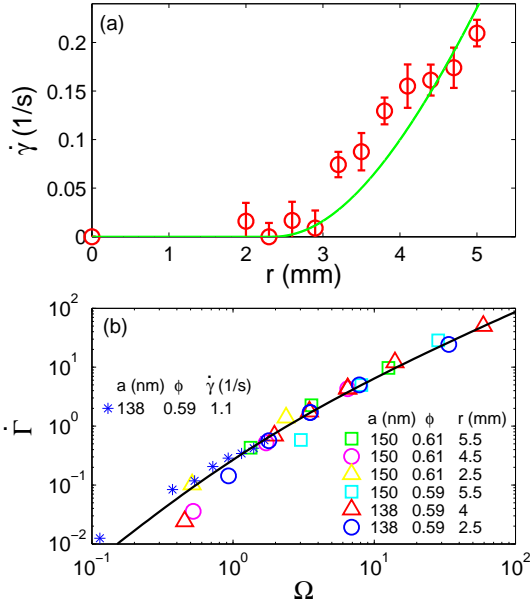


FIG. 3: (a) Local shear rate $\dot{\gamma}$, as determined from the velocity profiles, versus position r for $\dot{\gamma}_a = 1.1 \text{ s}^{-1}$, $a = 138 \text{ nm}$ and $\phi = 0.59$, the line is calculated from Eqs. (3) and (5). (b) Reduced local shear rate $\dot{\Gamma} = 2(\beta\theta r/\alpha)^2 \dot{\gamma}$ versus the reduced applied rate $\Omega = 2(\beta\theta/\alpha)^2 r(r - r_y) \dot{\gamma}_a$ in regime II, for two particle sizes a , various ϕ and distances r . The data in (a), at fixed $\dot{\gamma}_a$ but different r , are also represented in this plot (\star). Line: the prediction $\dot{\Gamma} = 1 + \Omega - \sqrt{1 + 2\Omega}$.

The local bulk shear rate $\dot{\gamma}(r)$ and $v_s(r)$ are related by:

$$\dot{\gamma}(r) = \dot{\gamma}_a - \frac{v_s(r)}{\theta r}. \quad (3)$$

We deduce the local flow behavior by equating, for each distance r , the stress in the bulk and at the wall. For $\sigma_s < \sigma(r) < \sigma_y$, $\dot{\gamma}(r) = 0$, full slip occurs and the stress is given by Eq. (1). Shear starts when the local shear stress $\sigma(r)$ induced by slip exceeds the yield stress σ_y , i.e., when $v_s \geq v_s^{(y)} = (\sigma_y - \sigma_s)/\beta$, which in a cone-plate geometry is equivalent to $r \geq r_y = (\sigma_y - \sigma_s)/(\beta\dot{\gamma}_a\theta)$. For $\sigma(r) > \sigma_y$ slip and shear are both present, and the stresses in Eqs. (1) and (2) must be equal. We can therefore calculate the measured shear stress σ_m using

$$\sigma_m = r_c^{-2} \int_0^{r_c} [\sigma_s + \beta v_s(r)] 2r dr, \quad (4)$$

with $v_s(r) = \dot{\gamma}_a \theta r$ for $r \leq r_y$ and

$$v_s(r) = \dot{\gamma}_a \theta r_y - \frac{\alpha^2}{2\beta^2 \theta r} \left[1 - \sqrt{1 + 4 \frac{\beta^2 \theta^2 \dot{\gamma}_a r}{\alpha^2} (r - r_y)} \right] \quad (5)$$

for $r > r_y$. The transition from regime I to II occurs when $r_y = r_c$, i.e. at $\dot{\gamma}_{a,c} = \frac{\sigma_y - \sigma_s}{\beta \theta r_c}$ and $\sigma_m = \frac{2\sigma_y + \sigma_s}{3} < \sigma_y$. Eq. (4) also gives the relation $\eta_{\text{eff}} = 2\beta\theta r_c/3$.

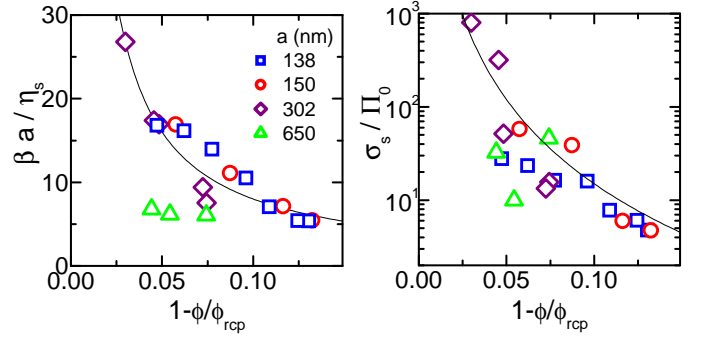


FIG. 4: (a) Normalized slip coefficient $\beta a/\eta_s$, versus reduced volume fraction $1 - (\phi/\phi_{\text{rcp}})$, for $a = 138 \text{ nm}$ (\square), 150 nm (\circ), 302 nm (\diamond), and 652 nm (\triangle). Full line: $\beta a/\eta_s = 0.8(1 - \phi/\phi_{\text{rcp}})^{-1}$. (b) The threshold stress σ_s , in units of $\Pi_0 = 3k_B T \phi / 4\pi a^3$, for different particle sizes (symbols as in (a)). Line: $\sigma_s/\Pi_0 = 0.015(1 - \phi/\phi_{\text{rcp}})^{-3}$.

To test this model, we extracted the parameters (β, σ_s) and (α, σ_y) from the smooth and rough wall flow curves respectively for various ϕ and a . Fig. 4 shows the volume fraction dependence of (β, σ_s). We return to their physical significance later. The theoretical predictions for the smooth-wall flow curves, calculated using Eq. (4) and the parameter values extracted from data, agree well with measurements; an example is shown in Fig. 1(b).

Additionally, Eqs. (3),(5) provide a reasonable description of the r -dependence of the local bulk shear rate $\dot{\gamma}$ for $r > r_y$, Fig. 3(a). We test the dependence of the local shear rate $\dot{\gamma}$ on $\dot{\gamma}_a$ by plotting the reduced local shear rate $\dot{\Gamma} = 2(\beta\theta r/\alpha)^2 \dot{\gamma}$ versus the reduced applied rate $\Omega = 2(\beta\theta/\alpha)^2 r(r - r_y) \dot{\gamma}_a$, Fig. 3(b). With this normalization, our model predicts a master curve $\dot{\Gamma} = 1 + \Omega - \sqrt{1 + 2\Omega}$. The data indeed follow this behavior for various concentrations, positions, and particle sizes, lending strong support for the validity of our model.

Summarizing thus far, a HS colloidal suspension driven along a smooth, non-stick wall exhibits slip for $\phi > \phi_g$, where the system acquires a finite yield stress. The global and local rheology at different concentrations and particle sizes in a cone-plate geometry are well described by a model in which the local stress and slip velocity are related by a Bingham form, Eq. 1, which should be applicable to flow of HS's in other geometries. Imaging the slip using the largest particles, Fig. 2, shows that we are *not* dealing with shear of a few layers of particles near the wall. We found the same result using a solvent that matches both the particle density and RI. Thus, gravity is irrelevant, and we expect for all particle sizes, the suspension slips as a solid body for $\sigma_s < \sigma < \sigma_y$.

The physical origins of the parameters β and σ_s in Eq. 1 are less clear. An obvious source for σ_s is van der Waals attraction [25]. But we minimised this by RI-matching. Removing RI-matching by using decalin as solvent, we observed no slip and $\sigma_m(\dot{\gamma}_a)$ shows the HB

form at all $\dot{\gamma}_a$ for $\phi > \phi_g$ [21], as with coated walls. Imaging dilute suspensions with $a = 652$ nm showed that in decalin particles were indeed stuck to the glass, while with RI matching such sticking was absent. We must therefore seek a different origin for σ_s in our system.

In an equilibrium HS fluid next to a wall, the contact value of the distribution function is proportional to the pressure [26]. There is little information for quiescent HS glasses next to walls [27]. Nevertheless, consistent with Fig. 2(a), we expect particle contacts in our system. We propose that σ_s reflects the Coulomb-like friction between particles in contact with the wall.

The osmotic pressure, $\Pi(\phi)$, may then play the role of ‘normal force’ in the Coulomb law, so we expect $\sigma_s \propto \Pi$. For HS glasses, Π is uncertain, but a widely used form is $\Pi = 2.9\Pi_0/(1 - \phi/\phi_{rcp})$ [28], with $\Pi_0 = 3\phi k_B T/(4\pi a^3)$ the ideal gas result. Thus σ_s/Π_0 should collapse data from different particle sizes, as is indeed the case, Fig. 4(b). But we also find $\sigma_s/\Pi_0 \sim (1 - \phi/\phi_{rcp})^\nu$ with $\nu \sim 2-3$, apparently inconsistent with simple Coulomb friction. However, our particles are polydisperse, and the colloidal glass is under finite shear strain during slip, so that the above form of $\Pi(\phi)$ may be inappropriate [29].

To predict the slip parameter β , we ideally should integrate the distribution of gap sizes between particles and wall with an appropriate form for the lubrication force [30]. Since the gap size distribution is poorly known for concentrated HS’s, we adopt a naive picture of a uniform lubrication layer with thickness $\xi = \eta_s/\beta$ [12]. Scaling this by the only natural length scale, a , collapses data for different particle sizes [31], Fig. 4(a), with ξ a small fraction of the particle size for all ϕ . Empirically, $\beta a/\eta_s = 0.8(1 - \phi/\phi_{rcp})^{-1} \simeq 0.28\Pi/\Pi_0$. We can calculate the average spacing between the first layer of particles and the wall, $\langle\delta\rangle$, by assuming that the contact value of the density $n(0)$ scales as Π and using for the density away from the wall, $n(z)$, a literature form known to be accurate for $\phi \lesssim 0.4$ [26]. This *equilibrium* estimate yields $\langle\delta\rangle/a \simeq \phi(1 - \phi/\phi_{rcp})^{-1} \simeq 0.23\Pi/\Pi_0$, strikingly close to our and previous [12] observations.

To conclude, we have demonstrated Bingham-like slip in concentrated HS suspensions above the glass transition. The apparent simplicity of the slip law, Eq. 1, however, emerges from the complex physics of HS glasses next to walls, which is not yet well understood, e.g. the structural consequences of small but finite strains below yielding. Our findings contrast strongly with observations in dense emulsions [7], showing that details matter in accounting for slip in soft glassy materials.

We thank A.B. Schofield for particles and M.E. Cates and A. Morozov for discussions. PB, RB and WP were funded by EPSRC grants EP/D067650, EP/D071070 and EP/E030173. LI was funded by the EU network MRTN-CT-2003-504712. GP acknowledges EU funding through

ToK ‘Cosines’ (MTC-D-CT-2005-029944) and NoE ‘Soft-Comp’ (NMP3-CT-2004-502235).

-
- [1] Y. Zhu and S. Granick, Phys. Rev. Lett. **87**, 096105 (2001); *ibid.*, **88**, 106102 (2002); J.L. Barrat and L. Bocquet, Phys. Rev. Lett. **82**, 4671 (1999).
 - [2] R.G. Larson, *The Structure and Rheology of Complex Fluids* (Oxford University Press, New York, 1999); H.A. Barnes, J. Non-Newtonian Fluid Mech. **56**, 221 (1995).
 - [3] A. Yoshimura and R.K. Prudhomme, J. Rheol. **32**, 53 (1988); W.B. Russel and M.C. Grant, Colloids Surf. A **161**, 271 (2000).
 - [4] R. Buscall *et al.*, J. Rheol. **37**, 621 (1993).
 - [5] H.M. Princen, J. Colloid Interface Sci. **105**, 150 (1985); D.M. Kalyon *et al.*, J. Rheol. **37**, 35 (1993);
 - [6] J.B. Salmon *et al.*, Eur. Phys. J. E **10**, 209 (2003).
 - [7] S.P. Meeker, R.T. Bonnecaze, and M. Cloitre, Phys. Rev. Lett. **92**, 198302 (2004); J. Rheol. **48**, 1295 (2004).
 - [8] L. Bécú *et al.*, Phys. Rev. Lett. **93**, 018301 (2004); *ibid.* **96**, 138302 (2006); Phys. Rev. E **76**, 011503 (2007).
 - [9] V. Bertola *et al.*, J. Rheol. **47**, 1211 (2003).
 - [10] G. Katgert *et al.*, cond-mat. 0711.4024.
 - [11] U. Yilmazer and D.M. Kalyon, J. Rheol. **33**, 1197 (1989).
 - [12] D.M. Kalyon, J. Rheol. **49**, 621 (2005).
 - [13] S.C. Jana *et al.*, J. Rheol. **39**, 1123 (1995).
 - [14] P.J. HartmanKok *et al.*, J. Col. Int. Sci **280**, 511 (2004).
 - [15] J.B. Salmon *et al.*, Eur. Phys. J. Appl. Phys. **22**, 143 (2003); S. Manneville *et al.*, Eur. Phys. J. Appl. Phys. **28**, 361 (2004); P. Coussot *et al.*, Phys. Rev. Lett. **88**, 218301 (2002); H. Wassenius and P.T. Callaghan, Eur. Phys. J. E **18**, 69 (2005).
 - [16] L. Isa *et al.*, Phys. Rev. Lett. **98**, 198305 (2007).
 - [17] I. Cohen *et al.*, Phys. Rev. Lett. **97**, 215502 (2006).
 - [18] G. Bryant *et al.*, Phys. Rev. E **66**, 060501 (2002).
 - [19] W. Schaertl and H. Sillescu, J. Stat. Phys. **77**, 1007 (1994).
 - [20] We checked that bending of the cover slide is negligible.
 - [21] G. Petekidis *et al.*, J. Phys. Cond. Mat. **16**, S3955 (2004).
 - [22] At high density $\phi \gtrsim 61\%$ and $1 < \sigma_m/\sigma_y \lesssim 1.2$, the velocity profiles with two rough walls show shear localization, to be reported elsewhere (manuscript in preparation).
 - [23] For $\phi \gtrsim 61\%$, before the complete vanishing of bulk shear ($v(z) = v_{\text{cone}}$), $v(z)$ starts to exhibit shear localization near the coated cone, in line with [22], while at the smooth glass we still find plug flow with $v_s \gtrsim 0.7v_{\text{cone}}$.
 - [24] R. Besseling *et al.*, Phys. Rev. Lett. **99**, 028301 (2007).
 - [25] J. R. Seth *et al.*, J. Rheol., *in press*, (2008).
 - [26] J.R. Henderson, F. van Swol, Mol. Phys. **51**, 991 (1984).
 - [27] C. R. Nugent *et al.*, Phys. Rev. Lett. **99**, 025702 (2007).
 - [28] L. V. Woodcock, Ann. N. Y. Acad. Sci. **37**, 274 (1983)
 - [29] Note that the normal stress of *sheared* HS’s scale as $(1 - \phi/\phi_{rcp})^{-3}\text{Pe}^2$ (where Pe is the Péclet number) (J. F. Brady and M. Vucic, J. Rheol. **39**, 545 (1995)), which has a ϕ scaling compatible with what we observe for σ_s ; but Pe = 0 in our slipping suspension.
 - [30] A.J. Goldman *et al.*, Chem. Eng. Sci. **22**, 637 (1967).
 - [31] For $\phi \lesssim 61\%$, the 652 nm batch showed slip and shear at small $\dot{\gamma}_a$, prohibiting reliable determination of β and σ_s .